한국해양공학회지 제17권 제3호, pp 1~6, 2003 (ISSN 1225-0767)

Application of Wavelet Transform to Problems in Ocean Engineering

SUN-HONG KWON*, HEE-SUNG LEE*, JUN-SOO PARK*
*Department of Naval Architecture and Ocean Engineering, Pusan National University, Busan, Korea

KEY WORDS: Wavelet Transform, Morlet Wavelet, Mexican-Hat Wavelet, Directional Wavelet, Directionality of Waves, Wave Profile, Decoupling of Signals

ABSTRACT: *This study presents the results of series of studies, which are mainly devoted to the application of wavelet transforms to various problems in ocean engineering. Both continuous and discrete wavelet transforms were used. These studies attempted to solve detection of wave directionality, detection of wave profile, and decoupling of the rolling component from free roll decay tests. The results of these analysis, using wavelet transform,demonstrated that the wavelet transform can be a useful tool in analyzing many problems in the filed of ocean engineering.*

1. Introduction

The wavelet transform is a powerful tool for solving a variety of physical problems. The advantage of wavelet transform, over traditional Fourier transform, lies in the fact that it provides information about time evolution, as well as frequency content of the signals, while the Fourier transform yields only frequency information.

The Fourier transform is a well-known frequency domain approach (Newland, 1993), which has been used, extensively, for frequency domain analysis, but it is not an appropriate tool for analyzing transient signals.

We discuss the concept of wavelet transform. Then the properties of Morlet and Mexican hat wavelet are described. To detect directionality, directional wavelet is adopted. The three examples of applications illustrated in this paper include detection of wave directionality by Morlet wavelet, detection of wave profile by Mexican wavelet, and decoupling of rolling component from free roll decay test data by discrete wavelet transform. The results of these analysis show that the wavelet transform has a potential to be utilized in signal analysis in fields of ocean engineering.

2. Wavelet Transform

First, the one-dimensional case of CWT(Continuous wavelet transform) is considered. A CWT of a signal $s(t)$ is given by

$$W_s(a,b)=\frac{1}{\sqrt{|a|}}\int_{-\infty}^{\infty}\psi^*\left(\frac{t-b}{a}\right)s(t)dt \tag{1}$$

where $\psi(\cdot)$ is the wavelet function, a is the scaling parameter, and b is the translation parameter. * represents a complex conjugate. It can be stated that the CWT is the sum over all time of real signal $s(t)$ multiplied by the scaled, shifted wavelet function. The parameters a and b vary continuously. For practical applications, the scale parameter a and the translation parameter b need to be discretized. This leads us to introduce DWT(Discrete wavelet transform). The theory of DWT is not reviewed here. Interested readers are referred to Daubechies (Daubechies, 1988, 1992).

3. Wavelets Used In This Study

We need to introduce wavelet functions to carry out wavelet transforms. The wavelet functions used in the present study are Morlet, Mexican hat and directional wavelet.

3.1 Morlet wavelet

The wavelet function used most often in the present analysis is Morlet wavelet. The formulation of this wavelet function is shown below

$$\psi(t)=\pi^{-\frac{1}{4}}(e^{-i\omega_0 t}-e^{-\frac{\omega_0^2}{2}})e^{-\frac{t^2}{2}} \tag{2}$$

The second term is added to satisfy the so-called

제1저자 권순홍 연락처: 부산광역시 금정구 장전2동 산30
051-510-2347 shkwon@pusan.ac.kr

admissibility condition. However, for large ω_0 ($\omega_0 \geq 5.5$), the correction term is numerically negligible. Thus the complex valued Morlet wavelet can be approximated by

$$\psi(t) = \pi^{-\frac{1}{4}} e^{-i\omega_0 t} e^{-\frac{t^2}{2}} \tag{3}$$

Fourier transform of this wavelet is of the form

$$\hat{\psi}(\omega) = \pi^{-\frac{1}{4}} e^{-\frac{(\omega-\omega_0)^2}{2}} \tag{4}$$

3.2 Mexican hat wavelet

The Mexican hat wavelet in one-dimensional space is of the following form.

$$\psi(x) = (1-x^2)e^{-x^2/2} \tag{5}$$

It is simply the second derivative of the Gaussian.

The two-dimensional Mexican hat function reads

$$\psi(\mathbf{x}) = (2-|\mathbf{x}|^2)\exp(-\frac{1}{2}|\mathbf{x}|^2) \tag{6}$$

The sharp slope and oscillating characteristics of the function enable us to detect discontinuities in the signal.

3.3 Directional wavelet

Rotation is introduced to detect directionality, as shown below

$$W_s(a,\theta,\mathrm{b}) = a^{-1}\int \psi^*(a^{-1}r_{-\theta}(\mathrm{x}-\mathrm{b}))s(\mathrm{x})d\mathrm{x} \tag{7}$$

where $r_{-\theta}(\mathrm{x}) = (x\cos\theta - y\sin\theta, x\sin\theta + y\cos\theta)$ at $0 \leq \theta < 2\pi$.

By introducing the rotation parameter, the wavelet function now has translation, rotation, and dilation. It is convenient to perform the two-dimensional DWT by using Parseval's theorem because the Fourier transform of $\psi(\mathrm{x})$ has compact support in the k domain.

$$W_s(a,\theta,\mathrm{b}) = a\int e^{i\mathrm{b}\cdot\mathrm{k}}\hat{\psi}^*(ar_{-\theta}(\mathrm{k}))\hat{s}(\mathrm{k})d\mathrm{k} \tag{8}$$

Where $\hat{\psi}$ and $\hat{s}$ are the Fourier transform of $\psi(\mathrm{x})$ and $s(\mathrm{x})$, respectively.

The Directional wavelet is favored for detecting wave directionality. Examples of directional wavelets are the Morlet wavelet, multi-directional wavelet, and the Cauchy wavelet (Antoine, 1996a, 1996b).

The formulation of a two-dimensional Morlet wavelet with rotation is given without a correction term, as follows

$$\psi(\mathbf{x}) = e^{i\mathbf{k}_0\cdot\mathbf{x}} e^{-\frac{1}{2}(\varepsilon^{-1}x^2+y^2)} \tag{9}$$

where k_0 is a wave vector and $\varepsilon \geq 1$ is an anisotropy parameter.

The expression for $\psi(\mathrm{x})$ adopted in the present study is given by

$$\psi(\mathbf{x}) = e^{ik_0 y} e^{-\frac{1}{2}(\varepsilon^{-1}x^2+y^2)} \tag{10}$$

Its Fourier transform is

$$\hat{\psi}(\mathrm{k}) = \sqrt{\varepsilon}\exp(-\tfrac{1}{2}(\varepsilon k_x^2 + (k_y - k_0)^2)) \tag{11}$$

4. Examples of Applications

4.1 Analysis of wave directionality (Kwon et. al. 2000)

For the substantial applications, data taken from video images were used. The video captured image presented in Fig. 1(a) has the direction of propagation 90. The picture was taken in a small water basin with water depth of about 45mm. Fig. 1(b) presents the distribution of 2-D wavelet transformed gray level. The directional analysis with k_0=10 and ε=10 shows the direction of propagation of the waves to be 90. The next image, which was also taken in the same water basin, features different direction of propagation, as can be clearly seen in Fig. 2(a). The direction of propagation was estimated as about 77. The result of the analysis is shown in Fig. 2(b). The results of the analysis seem quite accurate.

The image taken from the river is presented in Fig. 3(a). The waves shown in the figure have direction of propagation at 90. The main direction of propagation at 90 could be clearly detected from Fig. 3(b). Fig. 3(b) also reveals the fact that there exist many components of the waves. Oblique waves in the river are shown in Fig. 4. The directional wavelet transform clearly shows the main direction of the waves.

4.2. Analysis of 2D wave profile (Kwon et. al., 2002)

The experiment was done in small wave flume, whose dimensions were 4 m long, 0.3 m wide, and 0.6 m water depth. The waves are generated by a flap-type wave-maker. In all the experimental cases, the incoming wave height used was 6 cm. The two halogen lamps, located under the flume bottom, were used to illuminate the wave field.

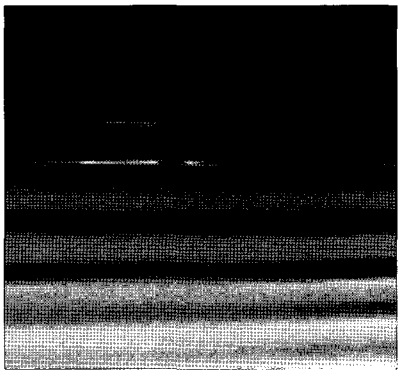

Fig. 1(a) Video image taken at small water basin

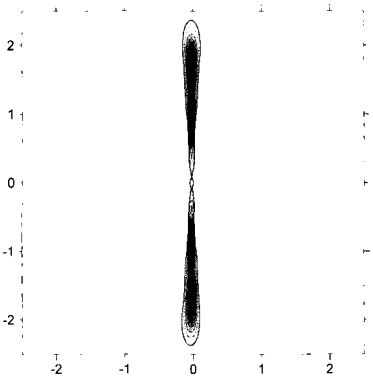

Fig. 1(b) 2-D directional wavelet transforms result

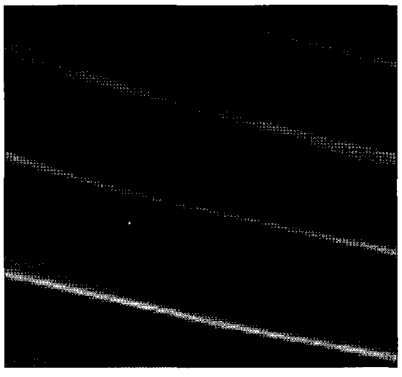

Fig. 2(a) Video image taken at small water basin

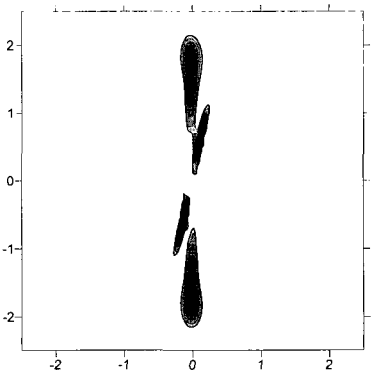

Fig. 2(b) 2-D directional wavelet transforms result

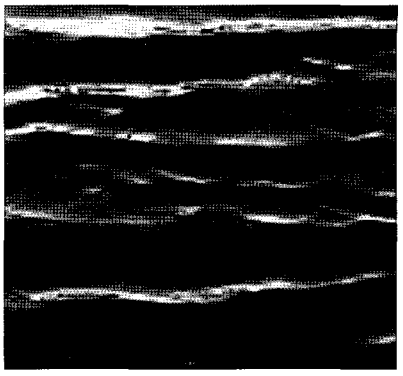

Fig. 3(a) Video image taken at river

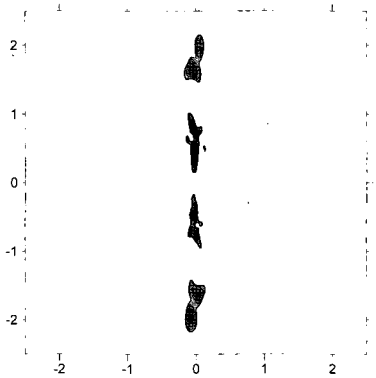

Fig. 3(b) 2-D directional wavelet transforms result

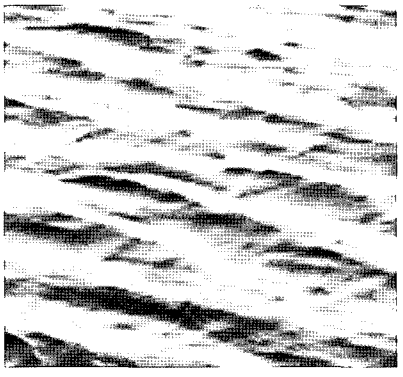

Fig. 4(a) Video image taken at river

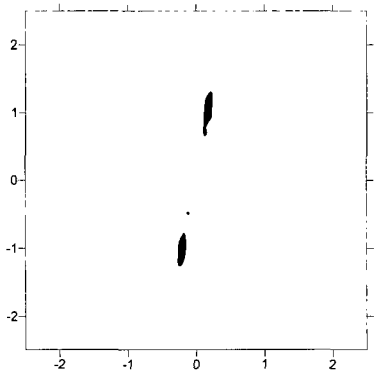

Fig. 4(b) 2-D directional wavelet transforms result

The regular wave recorded in Fig. 5 was analyzed yielding the result shown in Fig. 6. The numerical value 2^{-7} was selected for dilation parameter a after numerical experiments. The resolution of the image for the analysis was 640×480 meaning that the integration by eq. (6) had to be performed 640480 times. The integration was done by the trapezoidal rule. Irregular wave profiles, as shown in Fig. 7, were analyzed. The results are presented in Fig. 8.

To demonstrate the usefulness of the proposed study, the authors tried to apply the proposed scheme to the wave field disturbed by a submerged cylinder. Fig. 9 shows the wave field disturbed by the submerged cylinder. The wave field, when the crest was located at the center of the cylinder, is shown in Fig. 9. The analyzed profiles are shown in Fig. 10. The wave profiles were clearly detected, except at the breaking wave region. Those regions were interpolated. The central positions of the vertical width of the detected images in each column of the converted date were connected, which were assumed as free surfaces. The detected free surface is included in Fig. 10.

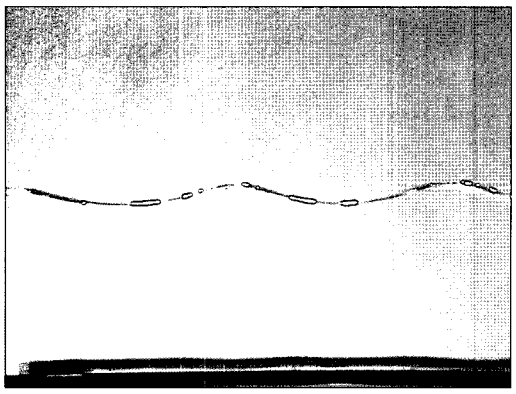

Fig. 5 Regular wave image

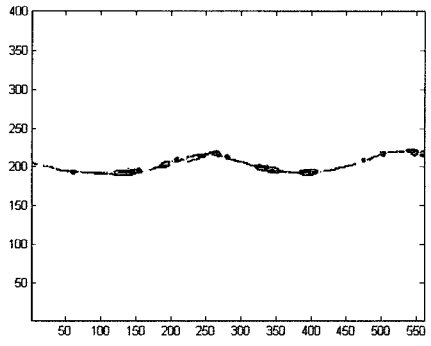

Fig. 6 Transformed image shown in Fig. 5

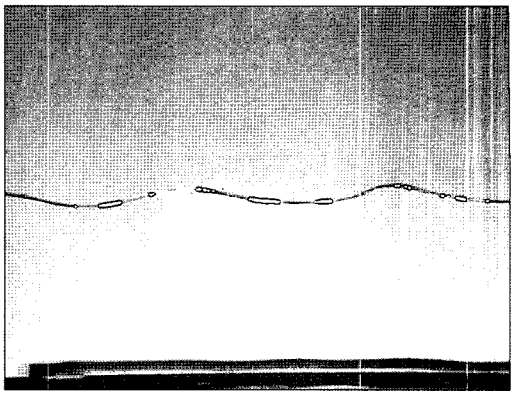

Fig. 7 Irregular wave profile image

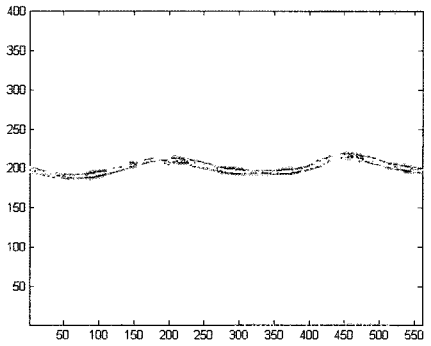

Fig. 8 Transformed image shown in Fig. 7

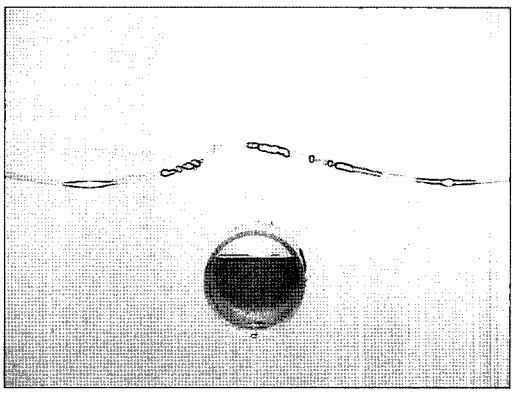

Fig. 9 Wave profile with a cylinder

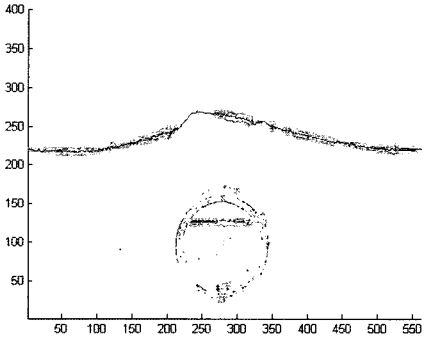

Fig. 10 Transformed image shown in Fig. 9

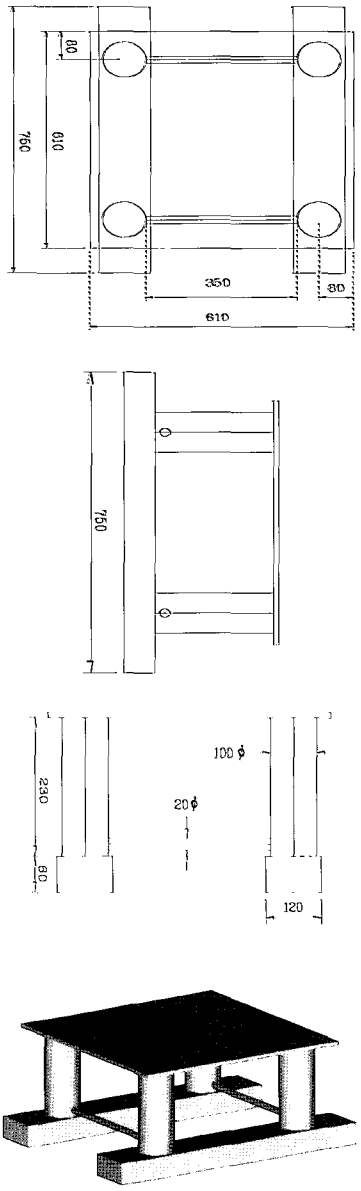

Fig. 11 Dimension and configuration of the model

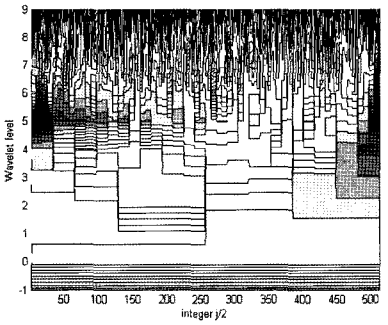

Fig. 13 The DWT map of raw data (db20 wavelet)

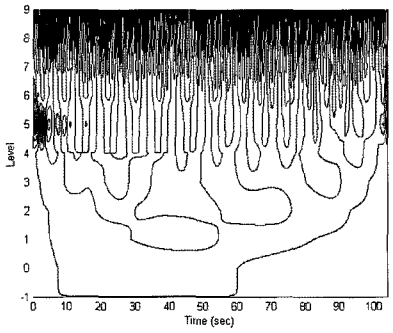

Fig. 14 The contour plot of raw data

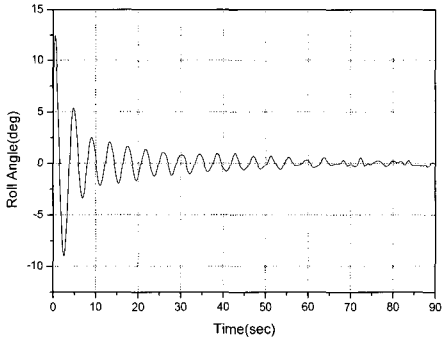

Fig. 15 Decoupled pure roll motion (level 4+level 5+level 6)

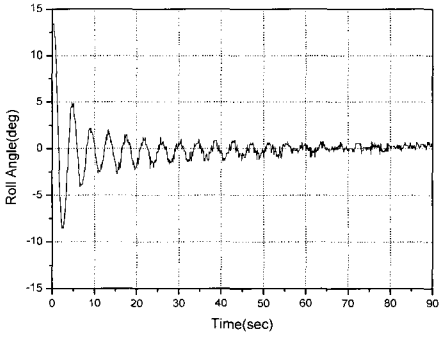

Fig. 12 Original data of roll decay taken by image processing

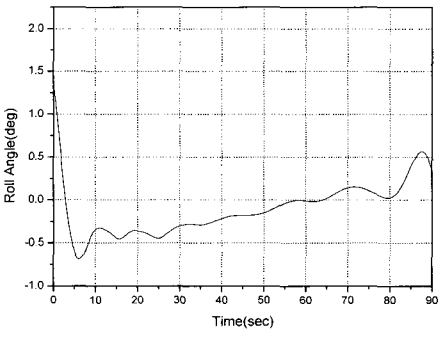

Fig. 16 Yaw effect (level 0 + level 1 + level 2 + level 3)

4.3 Decoupling method of signals (Kwon et. al., 2001)

The tested model was a semi-submersible pontoon-type offshore structure. The dimensions and the shape of the model are shown in Fig. 11. The units are in mm. The draft of the model was 170 mm and the initial roll angle for the test was 14. The model was completely free during the roll decay test.

The image processing technique was used to detect roll angle variation. Three points, used for detecting the roll angle, were marked on the model. The movements of these points were recorded with a video camera. By establishing the threshold values for suitable RGB values, these points could be detected. A computer program was developed to calculate the angles for every frame. The time history roll angle variation is shown in Fig. 12. It is evident that the signal is not a zero-mean process. Another notable problem was the presence of noise components in the signals. Wavelet transforms were used to solve the problem.

The DWT was applied to the signals. The results of the DWT are usually presented on a mean-square map, which is mainly designed to graphically illustrate the wavelet amplitudes squared by a three-dimensional plot. The details about the mean-square map can be found in Newland (1993). The mean-square map of the transformed Daubechies'20 coefficients is presented in Fig. 13. The height was plotted to a logarithmic scale, as shown in Fig. 13. The horizontal axis represents the translation in time, and the vertical axis represents the level of the DWT. We wanted to propose another method of illustration, which can be explained as follows. The separated signals were reconstructed. The results are presented in contour plots as shown in Fig. 14. The two sets of plots showed that the three major contributions of the signals can be clearly separated. Levels 7 through 9 were due to notice. Levels 4 through 6 were due to pure roll motion. Finally, levels 0 through 3 were thought to be due to a yaw effect. The reconstruction of the pure roll motion was easily accomplished by adding the signals from levels 4 through 6. The resulting pure roll motion and yaw motion are presented in Figs. 15 and 16, respectively. It can be seen that the vertical shift in the roll signal disappeared, as shown in Fig. 15. The straight line in Fig. 16 indicates the yaw angle variation as the roll motion continues. The decoupling of the two signals was successfully carried out by DWT.

5. Conclusions

The following conclusions are drawn from this study.

1. This study demonstrated that two-dimensional directional wavelet transforms can be efficient tools in the analysis of the directionality of waves when the related parameters are selected appropriately.
2. This study demonstrates that the Mexican hat function can be a useful tool in the analysis of wave profile
3. The DWT appears to be a very efficient tool for decoupling laboratory signals where time domain characteristics show transient behavior.

Acknowledgement

This work was supported by Pusan National University Research Grant, 1999.

References

Antoine, J.P. and Murenzi, R. (1996a). "Two-dimensional directional wavelets and the scale-angle representation", Signal Processing, Vol 52, pp 259-281.

Antoine, J.P. and Murenzi, R. (1996b). "The continuous wavelet transform, from 1 to 3 dimensions", in : Akansu, A.N. and Smith, M.J.T., eds., Subband and Wavelet Transforms. Design and Applications, pp 149-187.

Daubechies, I. (1988). "Orthogonal bases of compactly supported wavelets", Commun. on Pure and Appl. Math., Vol 41, pp 909-996.

Daubechies, I. (1992). "Ten lectures on wavelets", Society for Industrial and Applied Mathematics, Philadelphia, Pensylvania.

Kwon, S.H., Lee, H.S., Park, J.S. and HA, M.K. (2000). "On wavelet-based algorithm for interpreting ocean wave directionality", Proceedings of Fourth Osaka Colloquium on Seakeeping Performance of Ships, pp 237-241.

Kwon, S.H., Lee, H.S., Lee, H.S. and Ha, M.K. (2001). "Decoupling of free decay roll data by discrete wavelet transform", International Journal of Ocean Engineering and Technology, Vol 4, No 2, pp 14-18.

Kwon, S.H., Lee, H.S. and Jung, D.J. (2002). "Wave profile analysis by 2D Mexican hat wavelet transform", Proceedings of the Annual Spring Meeting, SNAK, pp 182-185.

Newland, D.E. (1993). An introduction to random vibrations, spectral and wavelet analysis, Third Edition, Longman Publication.

2003년 4월 10일 원고 접수
2003년 5월 14일 최종 수정본 채택